Available online at www.sciencedirect.com
SCIENCE DIRECT®
Computers & Fluids 34 (2005) 461–489
computers & fluids
www.elsevier.com/locate/compfluid

An efficient box-scheme for convection–diffusion equations with sharp contrast in the diffusion coefficients ☆

Jean-Pierre Croisille *, Isabelle Greff

Laboratoire de Mathématiques, Université de Metz, F-57045 Metz cedex, France

Received 15 January 2003; received in revised form 15 December 2003; accepted 31 December 2003
Available online 6 May 2004

Abstract

In this paper, we introduce a box-scheme for time-dependent convection–diffusion equations, following principles previously introduced by Courbet in [Rech. Aérospatiale 4 (1990) 21] for hyperbolic problems. This scheme belongs to the category of mixed finite-volume schemes. This means that it works on irregular meshes (finite-volume scheme) and computes simultaneously the principal unknown and its gradient in all Peclet regimes, ranging from pure diffusion ($Pe = 0$) to pure convection ($Pe = +\infty$). The present paper focuses mainly on the design of the scheme, which is non-standard, in the case of the 1D convection–diffusion equation. The version of the scheme presented here is of first or second order depending on the local Peclet number. We extend the 1D scheme afterwards in 2D by an ADI like technique. Several numerical results on 1D and 2D test-cases of interest for flow simulation in porous media are presented, some of them exhibiting sharp contrasts in diffusion coefficients.

1. Introduction

Originally introduced by Keller in [19] in the case of the heat equation, the design of the so called ''box-schemes'' has received interest in the 80s in different scientific communities in numerical computations. In particular, in compressible aerodynamics, several authors have addressed the extension of Keller's scheme to the Euler or Navier–Stokes compressible

☆ This work is supported by the G.D.R. MOMAS (CNRS) and the French National Agency for the Management of Radioactive Waste, (ANDRA).
* Corresponding author.
E-mail addresses: croisil@poncelet.univ-metz.fr (J.-P. Croisille), greff@poncelet.univ-metz.fr (I. Greff).

0045-7930/$ - see front matter
doi:10.1016/j.compfluid.2003.12.003

equations, [4,6,28,29]. However, these works reached only a limited audience due to the success of the finite-volume method based on Approximate Riemann Solvers, which is today the building block of most applied CFD softwares. There are several reasons for this. First, the basic design of box-schemes, which is at first similar to that of the finite-volume method, relies actually on a non-straightforward compatibility between the degrees of freedom and the discrete equations [5,7,9]. This is considered as a serious shortcoming of box-schemes. Second, box-schemes have no simple time-explicit versions, which is seen as a prohibitive drawback for hyperbolic problems. Finally, some box-schemes need for specific flow patterns, like "sonic" points or rarefaction waves, a special numerical tuning, [5]. Despite all these problems, box-schemes are still of great interest, because they are very accurate on poor meshes.

The box-scheme presented here is the generalization to time-dependent convection–diffusion equations of a box-scheme introduced in [7] for convection equations. In this paper, we emphasize both the construction of the scheme, and its application to linear convection–diffusion equations. The resulting scheme performs very well in the case of diffusion coefficients with large contrasts reaching values of as much as 10^6 or more. This is of interest e.g. for the numerical simulation of transport phenomena in porous media.

As in the elliptic (or parabolic) case, [10,11,13] the basic principle is to introduce the diffusive flux $p = -\varepsilon u_x$ as an auxiliary variable (mixed method) and to take the average of the conservation equation on one side, of the closure law of the diffusive flux on the other side on the same "boxes". In each of these averages, two upwind quadrature formulas are introduced, each one being designed to cure the well-known oscillations sources present in the approximation of convection–diffusion equations. The first one is a "time-independent" upwinding for the average of the diffusive flux $\bar{p}_K$ over a "box" K. This aims to prevent the spatial exponential instability at a stationary state $u(x)$, solution of $cu_x - \varepsilon u_{xx} = 0$, especially in boundary layers. This upwinding has been studied in the 1D stationary case in [11]. The second one is an upwind quadrature formula for the average $\bar{u}_K(t)$ of $u(x,t)$ over the box K. Its role is to give some control on the stable dispersive oscillations present in a centered discretization of the time-dependent convection–diffusion equation. Although the box-scheme we present here is only first order accurate at high Peclet number, we stress that it computes simultaneously the principal unknown and its gradient (or the diffusive flux), which corresponds to a higher order method in the principal unknown. For higher order versions, we refer to [12].

Let us mention finally that the box-scheme presented here has strong links with other numerical methods, in particular:

- High order finite difference compact schemes [2,20,24,26,30].
- Mixed finite element and SUPG methods [9–11,13].

The outline of the paper is as follows: after giving the notation in Section 2, we describe in Section 3 the design of the box-scheme for the 1D convection–diffusion equation, as well as some of its properties: stability, accuracy, numerical dissipation and dispersion. Afterwards, we explain in Section 4 how to extend this scheme to the 2D case by an ADI like algorithm. Finally, we present in Section 5 some numerical results for the 1D and 2D time-dependent convection–diffusion equation. This work has been announced in [14]. Additional information can be found in [18].

2. Notation

We consider the linear time-dependent convection–diffusion equation with constant coefficients in the segment $I =]0,1[$. Recall that this equation is

$$\begin{cases} u_t + cu_x - \varepsilon u_{xx} = f(x,t) \quad x \in I,\ t \geqslant 0 \\ u(x,0) = u_0(x) \\ u(0,t) = 0, \quad u(1,t) = 0 \end{cases} \tag{1}$$

The velocity is $c \in \mathbb{R}$ and the diffusion coefficient is $\varepsilon > 0$. We will consider the purely convective case $\varepsilon = 0$ as the limiting case $\varepsilon \to 0$. Therefore, we shall still use a scheme designed for convection–diffusion equation for a purely convection equation. We stress that this is performed only at the level of the *design* of the scheme and not as a artificial diffusion method. The notation for the discretization of the 1D equation is as follows: let the interval I be discretized by a finite element, possibly irregular mesh, with nodes $x_1 = 0 < x_2 < \cdots < x_N = 1$. We call $K_{j-1/2} = [x_{j-1}, x_j]$ a box, for $2 \leqslant j \leqslant N$. The size of the box $K_{j-1/2}$ is $h_{j-1/2} = x_j - x_{j-1}$. We make the quasi-uniformity hypothesis $Ch \leqslant h_{j-1/2} \leqslant h$, where $C > 0$ is a constant. We let $h_j = \frac{1}{2}(h_{j-1/2} + h_{j+1/2})$ and $h_1 = h_{3/2}/2$, $h_N = h_{N-1/2}/2$. The barycenter of the box $K_{j-1/2}$ is $x_{j-1/2} = \frac{1}{2}(x_j + x_{j-1})$. The coefficients α_j, β_j, $\bar{\alpha}_j$, $\bar{\beta}_j$, are defined by

$$\begin{cases} \alpha_j = h_{j-1/2}/h_j, \quad \bar{\alpha}_j = 1/\alpha_j, \quad 2 \leqslant j \leqslant N \\ \beta_j = h_{j+1/2}/h_j, \quad \bar{\beta}_j = 1/\beta_j, \quad 1 \leqslant j \leqslant N-1 \end{cases} \tag{2}$$

For any quantity Z_j^n, we note the incremental unknown

$$\delta Z_j^n = (Z_j^{n+1} - Z_j^n)/k \tag{3}$$

where $k = \Delta t$ is the time-step. Dimensionless cell numbers used in the sequel are

$$\begin{cases} \lambda_{j-1/2} = c\dfrac{k}{h_{j-1/2}} & \text{(Cell Courant number, } \lambda_{j-1/2} \in \mathbb{R}) \\ \mu_{j-1/2} = \varepsilon\dfrac{k}{h_{j-1/2}^2} & \text{(Cell diffusive number, } \mu_{j-1/2} > 0) \\ Pe_{j-1/2} = |c|\dfrac{h_{j-1/2}}{2\varepsilon} & \text{(Cell Peclet number, } Pe_{j-1/2} \geqslant 0) \end{cases} \tag{4}$$

The discrete unknowns are denoted by u_j^n, p_j^n and are respectively approximations of the principal unknown $u(x_j, t^n)$ and $p(x_j, t^n) = -\varepsilon u_x(x_j, t^n)$. The exact average operator onto the functions constant in each box $K_{j-1/2}$ is denoted by Π^0,

$$(\Pi^0 f)_{|K_{j-1/2}} = \frac{1}{h_{j-1/2}} \int_{x_{j-1}}^{x_j} f(x)\,\mathrm{d}x, \quad f \in L^2(I) \tag{5}$$

For any function $f(x)$, the notation $\bar{f}(x)$ will be used in the sequel for some approximation of $\Pi^0 f$ which depends on the context. The design of such approximations is the heart of the paper, as will become clear in Section 3.

3. A upwind box-scheme for the time-dependent convection–diffusion equation

3.1. Semi-discrete spatial box-scheme

We extend the design principles introduced by Courbet in [7], from the case of the convection equation $u_t + cu_x = 0$ to the convection–diffusion problem

$$\begin{cases} u_t + cu_x - \varepsilon u_{xx} = f(x,t) \\ u(0,t) = u(1,t) = 0 \\ u(x,0) = u_0(x) \end{cases} \tag{6}$$

We write (6) in mixed form by introducing the diffusive flux $p = -\varepsilon u_x$ as an auxiliary unknown

$$\begin{cases} u_t + cu_x + p_x = f(x,t) \quad t \geqslant 0 \\ p = -\varepsilon u_x \\ u(x,0) = u_0(x); \quad p(x,0) = -\varepsilon u_{0,x} \\ u(0,t) = u(1,t) = 0 \end{cases} \tag{7}$$

Integrating $(7)_1$, $(7)_2$ over the box $K_{j-1/2}$ yields the spatial semi-discrete relations, which hold at the level of the *exact solution*,

$$\begin{cases} \bullet \quad h_{j-1/2}\frac{\mathrm{d}}{\mathrm{d}t}\Pi^0 u_{|j-1/2}(t) + c[u(x_j,t) - u(x_{j-1},t)] \\ \qquad\qquad + [p(x_j,t) - p(x_{j-1},t)] = h_{j-1/2}(\Pi^0 f)_{|j-1/2}(t) \quad \text{(a)} \\ \bullet \quad h_{j-1/2}(\Pi^0 p)_{|j-1/2}(t) = -\varepsilon[u(x_j,t) - u(x_{j-1},t)] \quad \text{(b)} \\ \bullet \quad u(x_1,t) = u(x_N,t) = 0 \quad \text{(c)} \\ \bullet \quad u_j(0) = u_0(x_j) \quad \text{(d)} \end{cases} \tag{8}$$

Let us introduce now the semi-discrete unknowns $u_j(t)$, $p_j(t)$, approximating $u(x_j,t)$, $p(x_j,t)$. The semi-discrete box-scheme we consider is

$$\begin{cases} \frac{\mathrm{d}}{\mathrm{d}t}\bar{u}_{j-1/2}(t) + c[u_j(t) - u_{j-1}(t)]/h_{j-1/2} + [p_j(t) - p_{j-1}(t)]/h_{j-1/2} = \bar{f}_{j-1/2}(t) \quad \text{(a)} \\ \bar{p}_{j-1/2}(t) = -\varepsilon[u_j(t) - u_{j-1}(t)]/h_{j-1/2} \quad \text{(b)} \\ u_1(t) = u_N(t) = 0 \quad \text{(c)} \\ u_j(0) = u_0(x_j) \quad \text{(d)} \end{cases} \tag{9}$$

where $\bar{u}_{j-1/2}(t)$, $\bar{p}_{j-1/2}(t)$, are respectively approximations of $(\Pi^0 u)_{j-1/2}(t)$ and of $(\Pi^0 p)_{j-1/2}(t)$. In addition, $\bar{f}_{j-1/2}(t) \simeq (\Pi^0 f)_{j-1/2}(t)$. Let us stress that the cornerstone of box-schemes consists mainly into the definition of the two approximations of $(\Pi^0 u)_{j-1/2}(t)$ and $(\Pi^0 p)_{j-1/2}(t)$. We restrict ourselves in this paper to two-point quadrature formulas,

$$(\Pi^0 u)_{j-1/2}(t) \simeq Q_u(u_j(t), u_{j-1}(t)) \tag{10}$$

$$(\Pi^0 p)_{j-1/2}(t) \simeq Q_p(p_j(t), p_{j-1}(t)) \tag{11}$$

The closure quadrature formula (11) for the diffusive flux has been studied in [11] in the context of the time-independent convection–diffusion equation $cu_x - \varepsilon u_{xx} = f$. We keep for $\bar{p}_{j-1/2}(t)$ a formula like (54) in [11] of the form

$$\bar{p}_{j-1/2}(t) = \tfrac{1}{2}[p_j(t) + p_{j-1}(t)] - D_{p,j-1/2}(t)[p_j(t) - p_{j-1}(t)] \tag{12}$$

$D_{p,j-1/2}(t)$ is a piecewise constant function which aims to suppress any oscillating mode at the stationary state. A necessary condition is that $D_{p,j-1/2}c \geqslant 0$, (see (61) in [7,11]). For $\bar{f}_{j-1/2}(t)$, we simply take the exact formula $\bar{f}_{j-1/2}(t) = (\Pi^0 f(t))_{|j-1/2}$. For defining the approximate average value $\bar{u}_{j-1/2}$, we follow B. Courbet who introduced an upwind formula of the form [7]

$$\bar{u}_{j-1/2}(t) = \tfrac{1}{2}[u_j(t) + u_{j-1}(t)] + D_{u,j-1/2}(t)[u_j(t) - u_{j-1}(t)] \tag{13}$$

which plays a role only during the time-dependent phase. Let us consider now the time integration of $(9)_a$. The basic time scheme is here the ϑ-scheme, but higher order time schemes could be used, without changing the basic principles of the design, [8,12]. Integrating (9) in time by the ϑ-scheme yields the first equation of the box-scheme (recall that $\delta\bar{u}^n_{j-1/2} = \frac{\bar{u}^{n+1}_{j-1/2} - \bar{u}^n_{j-1/2}}{k}$)

$$\begin{aligned} h_{j-1/2}\delta\bar{u}^n_{j-1/2} = &-(1-\vartheta)c(u^n_j - u^n_{j-1}) - \vartheta c\left(u^{n+1}_j - u^{n+1}_{j-1}\right) - (1-\vartheta)(p^n_j - p^n_{j-1}) \\ &- \vartheta(p^{n+1}_j - p^{n+1}_{j-1}) + h_{j-1/2}\left((1-\vartheta)\bar{f}^n_{j-1/2} + \vartheta\bar{f}^{n+1}_{j-1/2}\right) \end{aligned} \tag{14}$$

Denoting the total flux $F^n_j = cu^n_j + p^n_j$, (14) may be rewritten

$$\delta\bar{u}^n_{j-1/2} = -\frac{1}{h_{j-1/2}}(F^n_j - F^n_{j-1}) - \frac{\vartheta k}{h_{j-1/2}}(c\delta u^n_j + \delta p^n_j - c\delta u^n_{j-1} - \delta p^n_{j-1}) + \mathscr{R}^n_{j-1/2}(f) \tag{15}$$

where the interpolation box operator $\mathscr{R}^n_{j-1/2}(f)$ is defined by

$$\mathscr{R}^n_{j-1/2}(f) = (1-\vartheta)\bar{f}^n_{j-1/2} + \vartheta\bar{f}^{n+1}_{j-1/2} \tag{16}$$

The incremental average $\delta\bar{u}^n_{j-1/2}$ is defined by the two points formula

$$\delta\bar{u}^n_{j-1/2} = \left(\frac{1}{2} + D^n_{u,j-1/2}\right)\delta u^n_j + \left(\frac{1}{2} - D^n_{u,j-1/2}\right)\delta u^n_{j-1} \tag{17}$$

Using this expression in (15) yields

$$\mathscr{L}^n_{j-1/2}(u,p) = \mathscr{R}^n_{j-1/2}(f) \tag{18}$$

where the box operator $\mathscr{L}^n_{j-1/2}$ defined in each box $K_{j-1/2}$ by

$$\begin{aligned} \mathscr{L}^n_{j-1/2}(u,p) = &\left[\frac{1}{2} + \vartheta\lambda_{j-1/2} + D^n_{u,j-1/2}\right]\delta u^n_j + \left[\frac{1}{2} - \vartheta\lambda_{j-1/2} - D^n_{u,j-1/2}\right]\delta u^n_{j-1} \\ &+ \frac{1}{h_{j-1/2}}(F^n_j - F^n_{j-1}) + \vartheta\frac{k}{h_{j-1/2}}(\delta p^n_j - \delta p^n_{j-1}) \end{aligned} \tag{19}$$

We consider now the discrete form of the constitutive law $(9)_b$. We select the coefficient $D_p(t)$ to be constant in time and in each box $K_{j-1/2}$ and denote it by $D_{p,j-1/2}$. At each time step t^n we have the relation

$$\left(\frac{1}{2} - D_{p,j-1/2}\right)p^n_j + \left(\frac{1}{2} + D_{p,j-1/2}\right)p^n_{j-1} = -\frac{\varepsilon}{h_{j-1/2}}(u^n_j - u^n_{j-1}) \tag{20}$$

Using the incremental variables δu^n_j, δu^n_{j-1}, δp^n_j, δp^n_{j-1}, (20) can be rewritten as, (subtract (20) at time n from (20) at time $n+1$),

$$k\vartheta\frac{\varepsilon}{h_{j-1/2}}(\delta u_j^n-\delta u_{j-1}^n)+k\vartheta\left(\frac{1}{2}-D_{p,j-1/2}\right)\delta p_j^n+k\vartheta\left(\frac{1}{2}+D_{p,j-1/2}\right)\delta p_{j-1}^n$$
$$=-\frac{\varepsilon}{h_{j-1/2}}(u_j^n-u_{j-1}^n)-\left(\frac{1}{2}-D_{p,j-1/2}\right)p_j^n-\left(\frac{1}{2}+D_{p,j-1/2}\right)p_{j-1}^n \tag{21}$$

Note that although the right-hand side term is zero in identity (21), we keep it for convenience in subsequent computations. Dividing by $h_{j-1/2}$, we get ($\mu_{j-1/2}=\varepsilon k/h_{j-1/2}^2$ in each box $K_{j-1/2}$)

$$\vartheta\mu_{j-1/2}(\delta u_j^n-\delta u_{j-1}^n)+\left(\frac{1}{2}-D_{p,j-1/2}\right)\frac{k\vartheta}{h_{j-1/2}}\delta p_j^n+\left(\frac{1}{2}+D_{p,j-1/2}\right)\frac{k\vartheta}{h_{j-1/2}}\delta p_{j-1}^n$$
$$=-\frac{\mu_{j-1/2}}{k}(u_j^n-u_{j-1}^n)-\frac{1}{h_{j-1/2}}\left\{\left(\frac{1}{2}-D_{p,j-1/2}\right)p_j^n+\left(\frac{1}{2}+D_{p,j-1/2}\right)p_{j-1}^n\right\}$$

Let us define the "box" operator $\mathscr{C}_{j-1/2}^n(u,p)$ by

$$\begin{aligned}\mathscr{C}_{j-1/2}^n(u,p)&=\vartheta\mu_{j-1/2}(\delta u_j^n-\delta u_{j-1}^n)+\frac{\mu_{j-1/2}}{k}(u_j^n-u_{j-1}^n)\\&\quad+\frac{1}{h_{j-1/2}}\left\{\left(\frac{1}{2}-D_{p,j-1/2}\right)p_j^n+\left(\frac{1}{2}+D_{p,j-1/2}\right)p_{j-1}^n\right\}\\&\quad+\left(\frac{1}{2}-D_{p,j-1/2}\right)\frac{k\vartheta}{h_{j-1/2}}\delta p_j^n+\left(\frac{1}{2}+D_{p,j-1/2}\right)\frac{k\vartheta}{h_{j-1/2}}\delta p_{j-1}^n\end{aligned} \tag{22}$$

Then, (21) may be rewritten

$$\mathscr{C}_{j-1/2}^n(u,p)=0 \tag{23}$$

Using (18) and (23), we obtain that the 1D box-scheme for the time-dependent convection–diffusion equation reads

$$\begin{cases}\mathscr{L}_j^n(u)=\mathscr{R}_j^n(f) & \text{(a)}\\ \mathscr{C}_{j-1/2}^n(u,p)=0 & \text{(b)}\end{cases} \tag{24}$$

Eqs. $(24)_a$ and $(24)_b$ are respectively a discretization of the conservation law and of the constitutive law of the diffusive flux. We eliminate now at the discrete level the diffusive flux p_j^n at the interface of the boxes $K_{j-1/2}$ and $K_{j+1/2}$. Recall that $h_j=\frac{1}{2}(h_{j-1/2}+h_{j+1/2}), 2\leqslant j\leqslant N$, with $h_1=h_{3/2}/2$, $h_N=h_{N-1/2}/2$. Let us define the values Y_j^n by

$$Y_j^n=\vartheta\frac{k}{h_j}\delta p_j^n \quad (\vartheta>0) \tag{25}$$

The following relations hold, (see (2))

$$\bar{\alpha}_j Y_j^n=\vartheta\frac{k}{h_{j-1/2}}\delta p_j^n;\quad \bar{\beta}_{j-1}Y_{j-1}^n=\vartheta\frac{k}{h_{j-1/2}}\delta p_{j-1}^n \tag{26}$$

Then, scheme (24) can be rewritten as the linear system in (Y_j^n, Y_{j-1}^n) consisting of (27) and (28)

$$\bar{\alpha}_j Y_j^n - \bar{\beta}_{j-1} Y_{j-1}^n = \mathscr{L}_{j-1/2}^n - \left(\frac{1}{2} + \vartheta\lambda_{j-1/2} + D_{u,j-1/2}^n\right)\delta u_j^n - \left(\frac{1}{2} - \vartheta\lambda_{j-1/2} - D_{u,j-1/2}^n\right)\delta u_{j-1}^n - \frac{1}{h_{j-1/2}}(F_j^n - F_{j-1}^n) \tag{27}$$

$$\begin{aligned}\left(\frac{1}{2} - D_{p,j-1/2}\right)\bar{\alpha}_j Y_j^n + \left(\frac{1}{2} + D_{p,j-1/2}\right)\bar{\beta}_{j-1} Y_{j-1}^n \\ = \mathscr{C}_{j-1/2}^n - \frac{\mu_{j-1/2}}{k}(u_j^n - u_{j-1}^n) - \frac{1}{h_{j-1/2}}\left\{\left(\frac{1}{2} - D_{p,j-1/2}\right)p_j^n + \left(\frac{1}{2} + D_{p,j-1/2}\right)p_{j-1}^n\right\} \\ - \vartheta\mu_{j-1/2}(\delta u_j^n - \delta u_{j-1}^n)\end{aligned} \tag{28}$$

Solving the 2×2 system (27) and (28) with unknowns (Y_j^n, Y_{j-1}^n) yields in box $K_{j-1/2}$

$$\begin{aligned}Y_j^n = \alpha_j\Bigg\{ &- \left[\vartheta\mu_{j-1/2} + \left(\frac{1}{2} + D_{p,j-1/2}\right)\left(\frac{1}{2} + \vartheta\lambda_{j-1/2} + D_{u,j-1/2}^n\right)\right]\delta u_j^n \\ &+ \left[\vartheta\mu_{j-1/2} - \left(\frac{1}{2} + D_{p,j-1/2}\right)\left(\frac{1}{2} - \vartheta\lambda_{j-1/2} - D_{u,j-1/2}^n\right)\right]\delta u_{j-1}^n \\ &- \frac{1}{k}\left[\mu_{j-1/2} + \lambda_{j-1/2}\left(\frac{1}{2} + D_{p,j-1/2}\right)\right][u_j^n - u_{j-1}^n] - \frac{1}{h_{j-1/2}}p_j^n \\ &+ \left(\frac{1}{2} + D_{p,j-1/2}\right)\mathscr{L}_{j-1/2}^n + \mathscr{C}_{j-1/2}^n\Bigg\}\end{aligned} \tag{29}$$

and

$$\begin{aligned}Y_{j-1}^n = \beta_{j-1}\Bigg\{ &- \left[\vartheta\mu_{j-1/2} + \left(\frac{1}{2} - D_{p,j-1/2}\right)\left(\frac{1}{2} + \vartheta\lambda_{j-1/2} + D_{u,j-1/2}^n\right)\right]\delta u_j^n \\ &+ \left[\vartheta\mu_{j-1/2} + \left(\frac{1}{2} - D_{p,j-1/2}\right)\left(\frac{1}{2} - \vartheta\lambda_{j-1/2} - D_{u,j-1/2}^n\right)\right]\delta u_{j-1}^n \\ &+ \frac{1}{k}\left[-\mu_{j-1/2} + \lambda_{j-1/2}\left(\frac{1}{2} - D_{p,j-1/2}\right)\right][u_j^n - u_{j-1}^n] - \frac{1}{h_{j-1/2}}p_{j-1}^n \\ &- \left(\frac{1}{2} - D_{p,j-1/2}\right)\mathscr{L}_{I,j-1/2}^n + \mathscr{C}_{j-1/2}^n\Bigg\}\end{aligned} \tag{30}$$

Identifying the two values of Y_j^n for $2 \leqslant j \leqslant N-1$ given by (29) in the box $K_{j-1/2}$ and by (30) in the box $K_{j+1/2}$ yields the three-point scheme

$$L_j^n(u) = \beta_j\left(\frac{1}{2} - D_{p,j+1/2}\right)\mathscr{L}_{j+1/2}^n + \alpha_j\left(\frac{1}{2} + D_{p,j-1/2}\right)\mathscr{L}_{j-1/2}^n - \beta_j\mathscr{C}_{j+1/2}^n + \alpha_j\mathscr{C}_{j-1/2}^n \tag{31}$$

where L_j^n is the three-point operator defined by

$$L_j^n(u) \stackrel{\text{def}}{=} a_j \delta u_{j+1}^n + b_j \delta u_j^n + c_j \delta u_{j-1}^n + c\left\{ \beta_j \left(\frac{1}{2} - D_{p,j+1/2} \right) \frac{u_{j+1}^n - u_j^n}{h_{j+1/2}} + \alpha_j \left(\frac{1}{2} + D_{p,j-1/2} \right) \frac{u_j^n - u_{j-1}^n}{h_{j-1/2}} \right\} - \frac{\varepsilon}{h_j} \left\{ \frac{u_{j+1}^n - u_j^n}{h_{j+1/2}} - \frac{u_j^n - u_{j-1}^n}{h_{j-1/2}} \right\} \tag{32}$$

In (32) the coefficients a_j, b_j and c_j are given by

$$\begin{cases} \bullet \quad a_j = \beta_j \left[-\vartheta \mu_{j+1/2} + \left(\frac{1}{2} - D_{p,j+1/2} \right) \left(\frac{1}{2} + \vartheta \lambda_{j+1/2} + D_{u,j+1/2}^n \right) \right] \\ \bullet \quad b_j = \beta_j \left[\vartheta \mu_{j+1/2} + \left(\frac{1}{2} - D_{p,j+1/2} \right) \left(\frac{1}{2} - \vartheta \lambda_{j+1/2} - D_{u,j+1/2}^n \right) \right] \\ \qquad\quad + \alpha_j \left[\vartheta \mu_{j-1/2} + \left(\frac{1}{2} + D_{p,j-1/2} \right) \left(\frac{1}{2} + \vartheta \lambda_{j-1/2} - D_{u,j-1/2}^n \right) \right] \\ \bullet \quad c_j = \alpha_j \left[-\vartheta \mu_{j-1/2} + \left(\frac{1}{2} + D_{p,j-1/2} \right) \left(\frac{1}{2} - \vartheta \lambda_{j-1/2} - D_{u,j-1/2}^n \right) \right] \end{cases} \tag{33}$$

Replacing the two box operators $\mathscr{L}_{j\pm\frac{1}{2}}^n$ and $\mathscr{C}_{j\pm\frac{1}{2}}^n$ by their values $\mathscr{L}_{j\pm\frac{1}{2}}^n = \mathscr{R}_{j\pm\frac{1}{2}}^n$ and $\mathscr{C}_{j\pm\frac{1}{2}}^n = 0$, we obtain the following point scheme

$$L_j^n(u) = R_j^n(f) \tag{34}$$

where L_j^n is given by (32) and R_j^n is the interpolation operator, (see (16))

$$R_j^n(f) = \beta_j \left(\frac{1}{2} - D_{p,j+1/2} \right) \mathscr{R}_{j+1/2}^n(f) + \alpha_j \left(\frac{1}{2} + D_{p,j-1/2} \right) \mathscr{R}_{j-1/2}^n(f) \tag{35}$$

The interest of (34) is that it makes apparent that the box-scheme can be written in the form of a compact finite difference scheme for the equation $u_t + cu_x - \varepsilon u_{xx} = f$, working on irregular mesh. (34) is actually a linear system in the incremental unknowns δu_j^n. In addition, once the values of δu_j^n are known, the values of δp_j^n are computed using (29) or (30).

We conclude this section by noting that the box-scheme has also the following non-incremental form (see Section 4)

$$(B - k\vartheta C)u^{n+1} = (B + k(1-\vartheta)C)u^n + kR^n(f) \tag{36}$$

which will be useful in the context of ADI like methods. The operator B, C are simply deduced from (32)–(34). They read, in the case where $D_{u,j-1/2}^n$ independent of n

$$(Bv)_j = \left\{ \beta_j \left[\frac{1}{2} - D_{p,j+1/2} \right] \left[\frac{1}{2} + D_{u,j+1/2} \right] \right\} v_{j+1} + \left\{ \beta_j \left[\frac{1}{2} - D_{p,j+1/2} \right] \left[\frac{1}{2} - D_{u,j+1/2} \right] + \alpha_j \left[\frac{1}{2} + D_{p,j-1/2} \right] \left[\frac{1}{2} + D_{u,j-1/2} \right] \right\} v_j + \left\{ \alpha_j \left[\frac{1}{2} + D_{p,j-1/2} \right] \left[\frac{1}{2} - D_{u,j-1/2} \right] \right\} v_{j-1} \tag{37}$$

and

$$
\begin{aligned}
(Cv)_j = &-\left\{\beta_j\left[-\frac{\varepsilon}{h_{j+1/2}^2}+\left(\frac{1}{2}-D_{p,j+1/2}\right)\frac{c}{h_{j+1/2}}\right]\right\}v_{j+1}\\
&-\left\{\beta_j\left[\frac{\varepsilon}{h_{j+1/2}^2}-\left(\frac{1}{2}-D_{p,j+1/2}\right)\frac{c}{h_{j+1/2}}\right]-\alpha_j\left[\frac{\varepsilon}{h_{j-1/2}^2}+\left(\frac{1}{2}+D_{p,j-1/2}\right)\frac{c}{h_{j-1/2}}\right]\right\}v_j\\
&-\left\{\alpha_j\left[\frac{-\varepsilon}{h_{j-1/2}^2}-\left(\frac{1}{2}+D_{p,j-1/2}\right)\frac{c}{h_{j-1/2}}\right]\right\}v_{j-1}
\end{aligned}
\tag{38}
$$

3.2. Finite difference analysis

In this section, we study the finite difference scheme resulting from the box-scheme (36) in the homogeneous case and with a constant meshsize $h_{j+1/2}=h$. In addition, we assume that $D^n_{u,j-1/2}=D_u$. With these assumptions, scheme (36) may be written

$$[B-k\vartheta C]u^{n+1}=[B+k(1-\vartheta)C]u^n \tag{39}$$

Equivalently, it can be expressed as the three-point implicit compact scheme

$$a_1u^{n+1}_{j+1}+a_0u^{n+1}_j+a_{-1}u^{n+1}_{j-1}=b_1u^n_{j+1}+b_0u^n_j+b_{-1}u^n_{j-1} \tag{40}$$

where the coefficients are (see (37) and (38) and recall that $\lambda=ck/h$; $\mu=\varepsilon k/h^2$)

$$
\begin{cases}
a_1=\left(\frac{1}{2}-D_p\right)\left(\frac{1}{2}+D_u+\vartheta\lambda\right)-\vartheta\mu\\
b_1=\left(\frac{1}{2}-D_p\right)\left(\frac{1}{2}+D_u-\lambda(1-\vartheta)\right)+\mu(1-\vartheta)\\
a_0=\frac{1}{2}+2\vartheta\mu+2D_p(D_u+\vartheta\lambda)\\
b_0=\frac{1}{2}-2(1-\vartheta)\mu+2D_p(D_u-(1-\vartheta)\lambda)\\
a_{-1}=\left(\frac{1}{2}+D_p\right)\left(\frac{1}{2}-D_u-\vartheta\lambda\right)-\vartheta\mu\\
b_{-1}=\left(\frac{1}{2}+D_p\right)\left(\frac{1}{2}-D_u+\lambda(1-\vartheta)\right)+\mu(1-\vartheta)
\end{cases}
\tag{41}
$$

The stability condition is deduced from a general result of Rigal, [23].

Proposition 3.1. *The scheme* (40) *and* (41) *is stable in the Von Neumann sense if and only if the two following conditions are fulfilled*

(i) $\widetilde{D}_u\lambda+\mu\geqslant 0$,
(ii) $[D_p\lambda+\mu]\left[\widetilde{D}_uD_p+\left(\vartheta-\frac{1}{2}\right)\mu\right]\geqslant 0$,

where $\widetilde{D}_u$ *denotes* $\widetilde{D}_u=D_u+(\vartheta-\frac{1}{2})\lambda$.

Proof. We apply the result of Rigal [23]. The amplification factor of scheme (40) is $g(\theta)=g_1(\theta)/g_2(\theta), \theta\in[0,2\pi[$, with

$$
\begin{cases}
g_1(\theta)=b_0+(b_1+b_{-1})\cos\theta+\mathrm{i}(b_1-b_{-1})\sin\theta\\
g_2(\theta)=a_0+(a_1+a_{-1})\cos\theta+\mathrm{i}(a_1-a_{-1})\sin\theta
\end{cases}
\tag{42}
$$

The necessary and sufficient condition in order to have the strong stability condition

$$\sup_{\theta\in[0,2\pi[} |g(\theta)| \leqslant 1 \tag{43}$$

is

$$a_1 + a_{-1} - b_1 - b_{-1} \leqslant \min[(a_1 - a_{-1})^2 - (b_1 - b_{-1})^2; (a_1 + a_{-1})^2 - (b_1 + b_{-1})^2] \tag{44}$$

One checks easily that this condition is equivalent to (i) + (ii). □

In [11], the following sufficient stability criterion has been derived in the case of the time-independent convection–diffusion equation

$$\mathrm{sgn}(c)\, D_p \geqslant \frac{1}{2} \max\left(0, 1 - \frac{1}{Pe}\right) \tag{45}$$

Using this result, we deduce that

Corollary 3.1. *A set of sufficient stability conditions is*

(i) $\mu + \lambda D_p \geqslant \frac{|\lambda|}{2}$ ((60) *in* [11]),
(ii) $\mu + \lambda \widetilde{D}_u \geqslant 0$,
(iii) $\widetilde{D}_u D_p + (\vartheta - \frac{1}{2})\mu \geqslant 0$.

3.3. Equivalent equation analysis

We extend now to the convection–diffusion case the equivalent equation analysis of [7,17]. If A is a linear spatial operator, of maximal order $\mathrm{O}(A)$, the equivalent equation of a scheme applied to an evolution equation

$$\frac{\mathrm{d}u}{\mathrm{d}t} = Au \tag{46}$$

is the (formal) equation

$$\frac{\mathrm{d}u}{\mathrm{d}t} = Au + \sum_{\alpha \geqslant \mathrm{O}(A)} h^\alpha E_{\alpha+1} \partial_{\alpha+1} u \tag{47}$$

obtained by performing the Taylor expansion of the scheme and by replacing all the time derivatives but one, by space derivatives with the help of the modified equation itself. For a more precise definition, we refer to [3,12].

Proposition 3.2. *Suppose that the velocity $c > 0$ and the Peclet number $Pe = \frac{|c|h}{2\varepsilon}$ are fixed. Then, the equivalent equation of the scheme* (40)

$$u_t + cu_x - \varepsilon u_{xx} = hE_2 u_{xx} + h^2 E_3 u_{xxx} + \cdots \tag{48}$$

is such that the first order dissipation coefficient E_2, and the second order dispersive coefficient E_3 are respectively given by ($\widetilde{D}_u = D_u + (\vartheta - 1/2)\lambda$)

$$E_2 = c\widetilde{D}_u; \quad E_3 = c\left[\frac{1}{12}(1-\lambda^2) - \widetilde{D}_u^2\right] - \frac{\varepsilon}{h}\left[\widetilde{D}_u + \left(\vartheta - \frac{1}{2}\right)\lambda - D_p\right] \tag{49}$$

Proof. A convenient way to compute the coefficient E_α is simply to use the connection between (47) and the amplification factor $g(\theta)$ given by,

$$g(\theta) = \mathrm{e}^{ks_h\left(\frac{\theta}{h}\right)} \tag{50}$$

where $s_h(\xi)$ is the symbol of the spatial operator $A_h u(x) = -cu_x + \varepsilon u_{xx} + \sum_{\alpha \geqslant 1} h^\alpha E_{\alpha+1}\partial_{\alpha+1}u$ given by

$$s_h(\xi) = -\mathrm{i}c\xi - \varepsilon\xi^2 + \sum_{\alpha \geqslant 1} h^\alpha E_{\alpha+1}(\mathrm{i}\xi)^{\alpha+1} \tag{51}$$

This connection has been pointed out in [3,17]. Replacing ξ by θ/h, we get

$$ks_h(\xi) = \ln g(\theta) = -\mathrm{i}\lambda\theta - \mu\theta^2 + \frac{k}{h}\sum_{\alpha \geqslant 1} \mathrm{i}^{\alpha+1}E_{\alpha+1}\theta^{\alpha+1} \tag{52}$$

The Taylor expansion of $\ln g(\theta)$ at $\theta = 0$ is obtained by $\ln\, g(\theta) = \ln g_1(\theta) - \ln g_2(\theta)$.

Taking into account that $a_{-1} + a_0 + a_1 = 1$ and $\ln(1+x) = x - \frac{x^2}{2} + \frac{x^3}{3} + \mathrm{O}(x^4)$, we obtain for $\ln\, g_{1,2}(\theta)$

$$\ln g_1(\theta) = B_1(\vartheta - 1)\theta + B_2(\vartheta - 1)\theta^2 + B_3(\vartheta - 1)\theta^3 + \mathrm{O}(\theta^4) \tag{53}$$

$$\ln g_2(\theta) = B_1(\vartheta)\theta + B_2(\vartheta)\theta^2 + B_3(\vartheta)\theta^3 + \mathrm{O}(\theta^4) \tag{54}$$

where $B_1(\vartheta)$, $B_2(\vartheta)$, $B_3(\vartheta)$ are functions whose exact expression is not needed in the sequel. This yields finally $\ln\, g(\theta) = A_1\theta + A_2\theta^2 + A_3\theta^3 + \mathrm{O}(\theta^4)$ with

$$\begin{cases} A_1 = -\mathrm{i}\lambda \\ A_2 = -\mu - \lambda\widetilde{D}_u; \quad A_3 = \mathrm{i}\left\{\lambda\left(\widetilde{D}_u^2 - \frac{1}{12}(1-\lambda^2)\right) + \mu\left(\widetilde{D}_u + \left(\vartheta - \frac{1}{2}\right)\lambda - D_p\right)\right\} \end{cases} \tag{55}$$

The symbol of the spatial part of the equivalent equation

$$u_t = -cu_x + (\varepsilon + hE_2)u_{xx} + h^2E_3u_{xxx} + \cdots \tag{56}$$

is

$$s_h(\xi) = -\mathrm{i}c\xi - (\varepsilon + hE_2)\xi^2 - \mathrm{i}h^2E_3\xi^3 + \cdots \tag{57}$$

Therefore

$$ks_h(\xi) = -\mathrm{i}\lambda\theta - \left(\mu + E_2\frac{k}{h}\right)\theta^2 - \mathrm{i}\frac{k}{h}E_3\theta^3 + \cdots \tag{58}$$

which yields

$$A_1 = -\mathrm{i}\lambda; \quad A_2 = -\mu - E_2\frac{k}{h}; \quad A_3 = -\mathrm{i}\frac{k}{h}E_3. \tag{59}$$

Replacing the coefficients A_2 and A_3 by their values (55), we deduce (49). □

In the asymptotic expansion (48), the hypothesis that the Peclet number $Pe = \frac{|c|h}{2\varepsilon}$ is kept constant, implies actually that $\varepsilon = \mathrm{O}(h) \to 0$, when $h \to 0$. Therefore, the effective total dissipation coefficient is $E_2 + \frac{\varepsilon}{h}$.

The equivalent equation is usually used to provide a tool for selecting parameters in finite difference schemes, [7,8,17], for example by minimizing the numerical dissipation and dispersion.

Here we limit ourselves to the following empirical tuning:

- D_p is selected according to [11]

$$D_p = \frac{1}{2}\mathrm{sgn}(c)\max\left(0, 1 - \frac{1}{Pe}\right) \tag{60}$$

  This value of D_p is based on the numerical analysis of the box-scheme for the time-independent convection–diffusion equation $cu_x - \varepsilon u_{xx} = f$, [11].
- D_u is selected according to the following empirical formula

$$D_u = \frac{1}{2}\mathrm{sgn}(c)\max\left(0, \frac{1}{Pe_0} - \frac{1}{Pe}\right) \tag{61}$$

  where the Peclet number is $Pe = |c|h/2\varepsilon$, and $Pe_0 \geqslant 1$ is some threshold Peclet number, which will be determined empirically. The sense of (61) is that when the time parameter $\vartheta = 1/2$, we have the two following cases:
  - If $Pe \geqslant Pe_0$, then the diffusion coefficient $E_2 = \frac{|c|}{2Pe_0}$ and the box-scheme is first order accurate.
  - If $Pe < Pe_0$, then $D_u = 0$, $E_2 = 0$ and the box-scheme is second order accurate.

  Note that, both D_u and D_p act on the numerical dispersion E_3 in (49). Formulas (60) and (61) are selected only for simplicity and are independent of the solution. We refer to [12] for more accurate formulas, acting as non-linear functions of the solution.

4. An ADI box-scheme for the 2D convection–diffusion equation

In this section, we describe how to extend the box-scheme (34) to regular 2D finite difference meshes by an ADI algorithm. Consider the 2D linear convection–diffusion equation

$$\begin{cases} u_t + c_1 u_x + c_2 u_y - \varepsilon(u_{xx} + u_{yy}) = f(x,y,t), \quad (x,y) \in \Omega =]0,1[^2 \\ u(x,y,t) = g(x,y,t), \quad (x,y) \in \Gamma_D \\ \frac{\partial u}{\partial n}(x,y,t) = h(x,y,t), \quad (x,y) \in \Gamma_N \end{cases} \tag{62}$$

where Γ_D and Γ_N stand for the Dirichlet and the Neumann part of the boundary. Define the x and y spatial operators by

$$A_1 u(x,y) = -(c_1 u_x - \varepsilon u_{xx}); \quad A_2 u(x,y) = -(c_2 u_y - \varepsilon u_{yy}) \tag{63}$$

The time ϑ-scheme for (62) may be written as

$$\begin{aligned}(I - k\vartheta A_1)(I - k\vartheta A_2)u^{n+1} = {} & (I + k(1-\vartheta)A_1)(I + k(1-\vartheta)A_2)u^n \\ & + k(\vartheta f^{n+1} + (1-\vartheta)f^n) + \mathrm{O}(k^2)\end{aligned} \tag{64}$$

with an $O(k^3)$ error term, if $\vartheta = 1/2$. We approximate now the operator $I - k\vartheta A_1$ by $I - k\vartheta A_x$, where $A_x = B_x^{-1}C_x$, and where B_x and C_x are the box operators in the direction x defined in (37) and (38). Approximating similarly $I - k\vartheta A_2$ by $I - k\vartheta A_y$, with $A_y = B_y^{-1}C_y$, we obtain the following ADI version of the box-scheme

$$[I - k\vartheta B_x^{-1}C_x][I - k\vartheta B_y^{-1}C_y]u^{n+1} = [I + k(1-\vartheta)B_x^{-1}C_x][I + k(1-\vartheta)B_y^{-1}C_y]u^n + k[\vartheta f^{n+1}(1-\vartheta)f^n] \tag{65}$$

We check readily that u^{n+1} can be obtained by the two step Peaceman–Rachford factorization algorithm, [15,16,22,25]:

$$\begin{cases} (I - k\vartheta A_x)\tilde{u} = [I + k(1-\vartheta)A_y]u^n + k\vartheta[\vartheta f^{n+1} + (1-\vartheta)f^n] & \text{(a)} \\ (I - k\vartheta A_y)u^{n+1} = [I + k(1-\vartheta)A_x]\tilde{u} + k(1-\vartheta)[\vartheta f^{n+1} + (1-\vartheta)f^n] & \text{(b)} \end{cases} \tag{66}$$

Eq. $(66)_a$ shows that operator $I - k\vartheta A_x$ acts only on the horizontal components $(u_{i,j_0})_{2 \leqslant i \leqslant N_x - 1}$, $2 \leqslant j_0 \leqslant N_x - 1$. The operator $I - k\vartheta A_y$ acts only on the vertical components $(u_{i_0,j})_{2 \leqslant j \leqslant N_y - 1}$, with $2 \leqslant i_0 \leqslant N_x - 1$. Let us describe now how to handle boundary conditions in the context of scheme (64).

- *Dirichlet boundary conditions*

For Dirichlet boundary conditions $u^n_{i_0,j_0} = g^n(x_{i_0}, y_{j_0})$ at boundary points, we simply specify explicitly the exact value of $u^{n+1}_{i_0,j_0} = g^{n+1}(x_{i_0}, y_{j_0})$ in $(66)_b$, at the correct position in vector $u^n_{i,j}$. A classical question concerning the ADI scheme is to know which value should be affected in the intermediate value $\tilde{u}$ on the boundary. Subtracting $(66)_b$ from $(66)_a$, we deduce

$$[(I - k\vartheta A_x) + (I + k(1-\vartheta)A_x)]\tilde{u} = [I + k(1-\vartheta)A_y]u^{n+1} + [I - k\vartheta A_y]u^n + k(2\vartheta - 1)[\vartheta f^{n+1} + (1-\vartheta)f^n] \tag{67}$$

Since operators A_x and A_y do not act on boundary points, we have the following identity for boundary values $\tilde{u}_\partial$. (∂ denotes any couple (i,j) such that $x_{i,j} \in \Gamma = \partial\Omega$.)

$$\tilde{u}_\partial = \frac{1}{2}(u^n_\partial + u^{n+1}_\partial) + k\left(\vartheta - \frac{1}{2}\right)(\vartheta f^{n+1}_\partial + (1-\vartheta)f^n_\partial) \tag{68}$$

This value is applied in the intermediate state.

- *Neumann boundary conditions*

In order to put $\frac{\partial u}{\partial \nu}^{n+1} = h^{n+1}$ at boundary points in scheme (65), we use the local reconstruction formula (30), expressing the diffusive flux as a function of the unknown u. We give the result in the case where the boundary point is the left point x_1 of the box $K_{3/2} = [x_1, x_2]$. The exterior normal is $\nu = -(1,0)$. We deduce easily from (30) the identity linking u_1^{n+1}, u_2^{n+1} to the value of the diffusive flux at the boundary $p_1^n = \varepsilon h(x_1, t^n)$, $p_1^{n+1} = \varepsilon h(x_1, t^{n+1})$, supposed to be known by the Neumann data on Γ_N.

$$\left[\vartheta\mu_{3/2}+\left(\frac{1}{2}-D_{p,3/2}\right)\left(\frac{1}{2}-\vartheta\lambda_{3/2}-D_{3/2}\right)\right]u_1^{n+1}-\left[\vartheta\mu_{3/2}-\left(\frac{1}{2}-D_{p,3/2}\right)\left(\frac{1}{2}+\vartheta\lambda_{3/2}+D_{3/2}\right)\right]u_2^{n+1}$$
$$=\vartheta\frac{k}{h_{3/2}}p_1^{n+1}+(1-\vartheta)\frac{k}{h_{3/2}}p_1^n-\left[(1-\vartheta)\mu_{3/2}-\left(\frac{1}{2}-D_{p,3/2}\right)\left(\frac{1}{2}+(1-\vartheta)\lambda_{3/2}-D_{3/2}\right)\right]u_1^n$$
$$+\left[(1-\vartheta)\mu_{3/2}-\left(\frac{1}{2}-D_{p,3/2}\right)\left(\frac{1}{2}-(1-\vartheta)\lambda_{3/2}+D_{3/2}\right)\right]u_2^n+k\left(\frac{1}{2}-D_{p,3/2}\right)\mathscr{R}_{3/2}^n \tag{69}$$

5. Numerical results

5.1. Introduction

The aim of this section is to demonstrate the efficiency of the box-scheme on convection–diffusion problems having sharp contrasts in the diffusion coefficients. Let us stress the following points: first, although the box-scheme designed in the preceding section is only first order accurate for high Peclet numbers, (see (61)), the observed accuracy is greater than 1 in certain cases. Second, the box-scheme provides simultaneously approximations of both u and of the gradient u_x, allowing higher order reconstructions in u. This kind of reconstruction is not studied further here. Finally, the main interest of the box-scheme is that the same principle holds for convection equations and for the convection–diffusion equation. This is not the case in the classical finite-volume methods where different numerical flux formulas are used depending on the nature of the flux, convective or diffusive. Let us stress finally that the parameters of the scheme are used in practice locally in each box, if the mesh is irregular.

5.2. Monodimensional test-cases

5.2.1. First test-case

We compare the numerical solution of the constant coefficient convection–diffusion problem defined on the half line, $x>0$.

$$\begin{cases} u_t+cu_x-\varepsilon u_{xx}=0, \quad x>0,\ c\in\mathbb{R},\ \varepsilon>0 \\ u(x,0)=0, \quad x>0 \\ u(0,t)=1, \quad u(+\infty,t)=0 \end{cases} \tag{70}$$

The exact solution is

$$u(x,t)=\frac{1}{2}\left[\operatorname{erfc}\left(\frac{x-ct}{2\sqrt{\varepsilon t}}\right)+\exp\left(\frac{cx}{\varepsilon}\right)\operatorname{erfc}\left(\frac{x+ct}{2\sqrt{\varepsilon t}}\right)\right] \tag{71}$$

We have plotted in Figs. 1, 3 and 5, the exact and computed solutions (u,u_x) with the box-scheme (34) at time $T=0.4$ with a 200 box irregular mesh. The diffusion coefficients are respectively $\varepsilon=0.02, 0.005, 0.001$ and the velocity is $c=1$. We plot in addition in Figs. 2, 4 and 6, the local Peclet number $Pe_{j-1/2}$, which varies strongly, due to the irregularity of the mesh. As

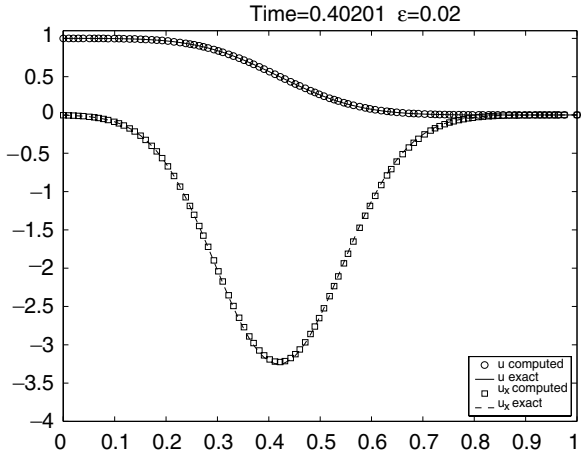

Fig. 1. Solution of problem (70), $T = 0.4$, $\varepsilon = 0.02$.

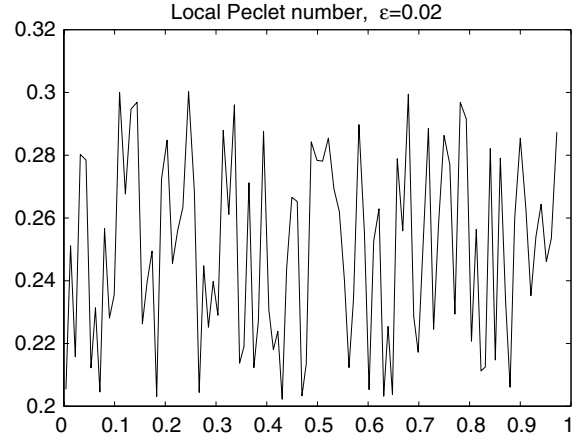

Fig. 2. Local Peclet number of problem (70), $T = 0.4$, $\varepsilon = 0.02$.

expected, we observe a very good agreement between the exact solution and the computed solution in the two first cases.

The parameters of the box-scheme are $\vartheta_{j-1/2} = 0.55$, $D_{p,j-1/2} = \frac{1}{2}\mathrm{sgn}(c)\max(0, 1 - \frac{1}{Pe_{j-1/2}})$, $D_{u,j-1/2} = \frac{1}{2}\mathrm{sgn}(c)\max(0, \frac{1}{Pe_0} - \frac{1}{Pe_{j-1/2}})$ with a threshold Peclet number $Pe_0 = 2.5$, see (61). In the last case, $\varepsilon = 0.001$, we have a convection dominated case and the scheme begins to show a lack of accuracy, particularly for the gradient u_x. In Table 1, we display the convergence rates obtained for u and the diffusive flux $p = -\varepsilon u_x$ in each of the three cases $\varepsilon = 0.02$, $\varepsilon = 0.005$ and $\varepsilon = 0.001$. This rate is the L^2 convergence rate α where $|u - u_h|_{L^2[0,1]} \leqslant Ch^\alpha$. We display the convergence rate estimated for the pair of meshes 50/100 boxes and 100/200 boxes. The results are very good in the three cases. Note that in the third case, the Peclet number begins to be located above the

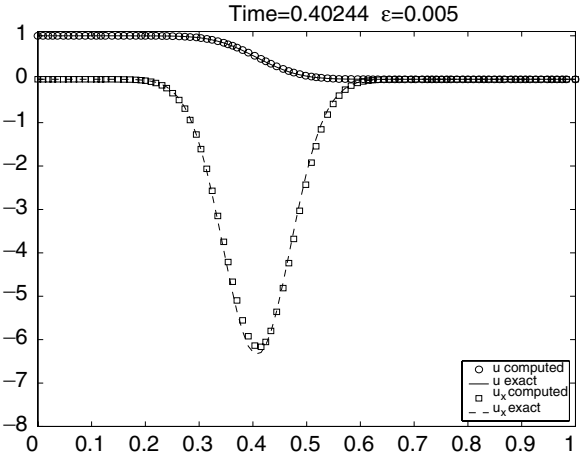

Fig. 3. Solution of problem (70), $T = 0.4$, $\varepsilon = 0.005$.

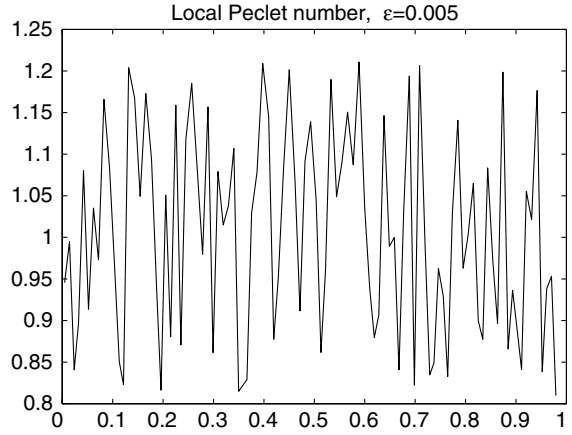

Fig. 4. Local Peclet number of problem (70), $T = 0.4$, $\varepsilon = 0.005$.

threshold Peclet number, causing the box-scheme to have a stronger artificial diffusion (upwind parameter D_u). However, the convergence rates are still good for u and $p = -\varepsilon u_x$. If we select a smaller diffusion coefficient ε, the scheme shows, as does every first order scheme, a more noticeable lack of accuracy. A less crude tuning than (60) and (61), will be presented in future works, [12].

5.2.2. Second test-case

In this second test-case, we demonstrate that the capabilities of the box-scheme are potentially very good on "real" problems, namely ones where sharp contrasts occur in the diffusion coefficients. The test-case consists of the following convection–diffusion equation, [14]

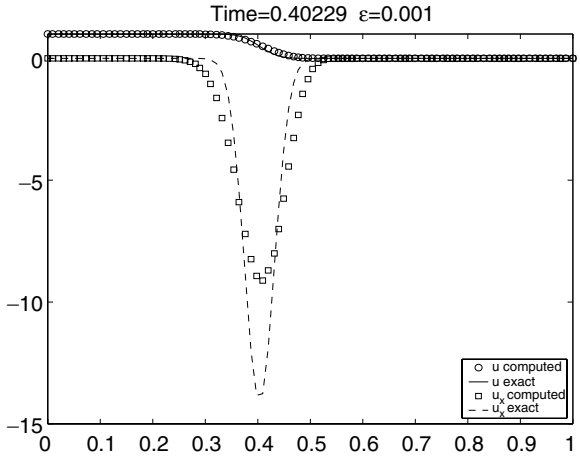

Fig. 5. Solution of problem (70), $T = 0.4$, $\varepsilon = 0.001$.

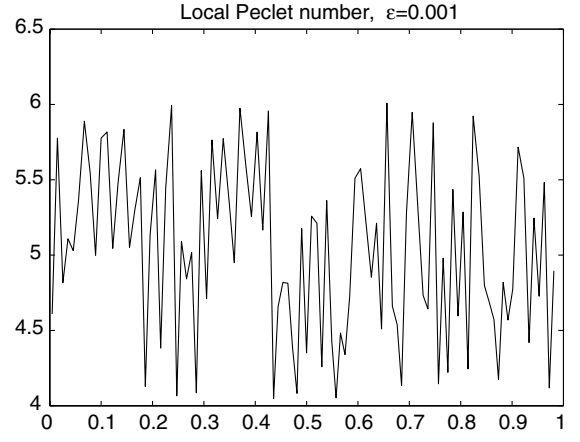

Fig. 6. Local Peclet number of problem (70), $T = 0.4$, $\varepsilon = 0.001$.

$$\begin{cases} u_t + u_x - (\varepsilon(x)u_x)_x = 0, & x \in [0,1] \\ u(x,0) = 0, & x \in]0,1] \\ u(0,t) = 1, & u(1,t) = 0 \end{cases} \tag{72}$$

where the diffusion coefficient is

$$\varepsilon(x) = \begin{cases} 10^{-6} & 0 < x < 0.15 \\ 1 & 0.15 < x < 0.25 \\ 10^{-3} & 0.25 < x < 0.35 \\ 10^{-1} & 0.35 < x < 0.45 \\ 1 & 0.45 < x < 1 \end{cases}$$

Table 1
Table of convergence rate for the first test-case (70)

Diff. coefft.	Conv. rate (u), 50/100 and 100/200	Conv. rate ($p = -\varepsilon u_x$), 50/100 and 100/200
$\varepsilon = 0.02$	1.57, 1.38	1.68, 1.11
$\varepsilon = 0.005$	1.68, 1.40	1.29, 1.25
$\varepsilon = 0.001$	0.90, 1.78	0.61, 1.90

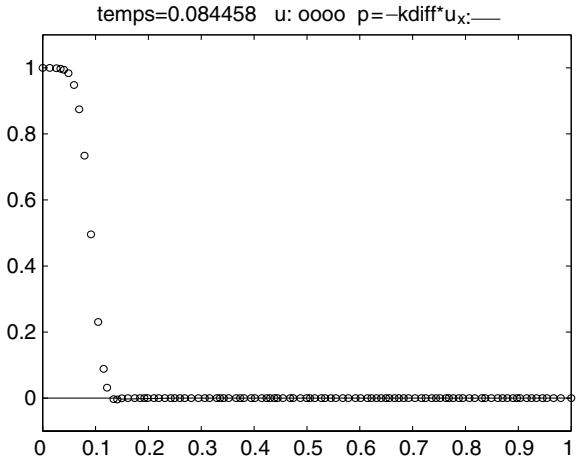

Fig. 7. Problem (72), Time $= T_1$, 100 boxes.

We display in Figs. 7–12 the values of $u(x)$ (circles), $p(x) = -\varepsilon u_x$ (straightlines) at the six times $T_1 = 0.084$, $T_2 = 0.175$, $T_3 = 0.238$, $T_4 = 0.35$, $T_5 = 0.525$ and $T_6 = 1.519$. The mesh is irregular (a finite-volume mesh) in order to prove that the scheme works like a finite-volume scheme. The value of the time integration parameter is $\vartheta = 0.5$. We have 100 boxes. The parameters $D_{u,j-1/2}$, $D_{p,j-1/2}$ are selected independently in each box according to (60) and (61). The threshold Peclet number in (60) has been fixed at $Pe_0 = 2.5$. The most interesting point is that there is no numerical dispersion, and that the profiles are perfectly monotonic. However, note that one can check numerically that the scheme does not formally satisfy a maximum principle: dispersive oscillations can occur during a very short transient elapse of time at the beginning of the computation. In all our computations, this problem can be avoided if necessary [1] by simply forcing u_j^{n+1} to belong to the physical interval of admissibility.

In Table 2, we give the convergence rates in the L^2 norm, for u and the diffusive flux $p = -\varepsilon u_x$ at the six times T_k, $1 \leqslant k \leqslant 6$. The exact solution is taken to be the numerical solution obtained with a 1024 point mesh. We report in Table 2 the convergence rates between a mesh of 50 boxes and 100 boxes on one hand, and between a mesh of 100 and 200 boxes on the other hand. As expected from the equivalent equation analysis, the scheme is first order accurate for u and for p. This is

[1] This is the case for example, for the computation of quantities like concentrations or temperature that should belong to a fixed interval.

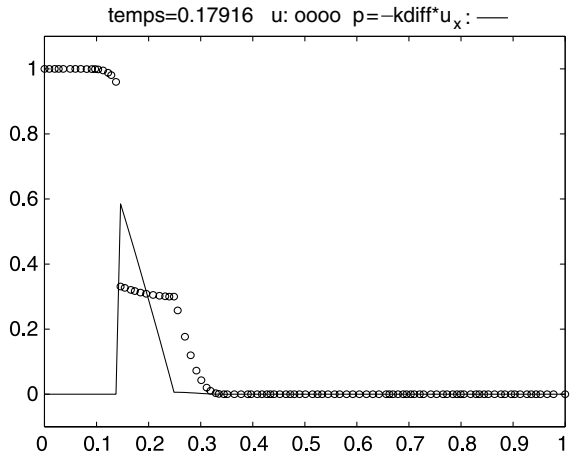

Fig. 8. Problem (72), Time $= T_2$, 100 boxes.

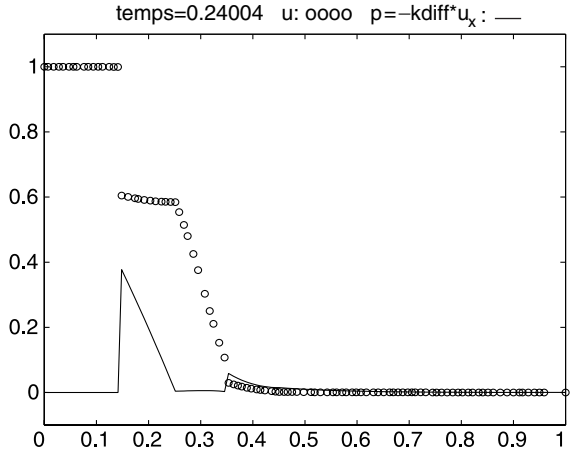

Fig. 9. Problem (72), Time $= T_3$, 100 boxes.

better than a standard first order non-mixed upwind scheme, in which there is no simultaneous computation of the diffusive flux. Note that a mesh of 100 or 200 boxes is a small mesh for such a case.

5.3. 2D problems

5.3.1. Introduction

In this part, we solve a convection diffusion problem with our ADI box-scheme for two academic examples. In all cases, the time integration parameter $\vartheta = \frac{1}{2}$. The upwind coefficients in the directions x and y are $D_{u,x}$, $D_{p,x}$ and $D_{u,y}$, $D_{p,y}$. They are computed by the 1D formulas

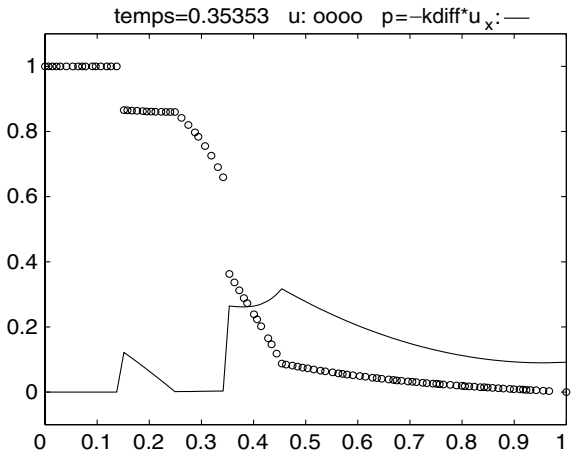

Fig. 10. Problem (72), Time $= T_4$, 100 boxes.

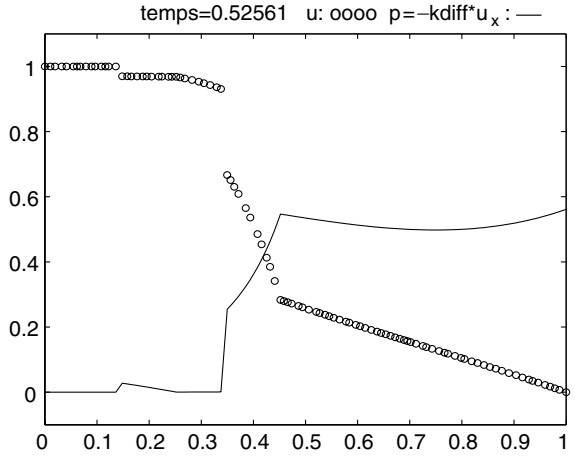

Fig. 11. Problem (72), Time $= T_5$, 100 boxes.

$$\begin{cases} D_{p,x,j-1/2} = \frac{1}{2}\operatorname{sgn}(c_1)\max\left(0, 1 - \frac{1}{Pe_{x,j-1/2}}\right) \\ D_{u,x,j-1/2} = \frac{1}{2}\operatorname{sgn}(c_1)\max\left(0, \frac{1}{Pe_0} - \frac{1}{Pe_{x,j-1/2}}\right) \\ D_{p,y,j-1/2} = \frac{1}{2}\operatorname{sgn}(c_2)\max\left(0, 1 - \frac{1}{Pe_{y,j-1/2}}\right) \\ D_{u,y,j-1/2} = \frac{1}{2}\operatorname{sgn}(c_2)\max\left(0, \frac{1}{Pe_0} - \frac{1}{Pe_{y,j-1/2}}\right) \end{cases} \tag{73}$$

where $\vec{c}(c_1, c_2)$ is the velocity and $Pe_{x,j-1/2}$, $Pe_{y,j-1/2}$ are the edge Peclet numbers in the x and y directions.

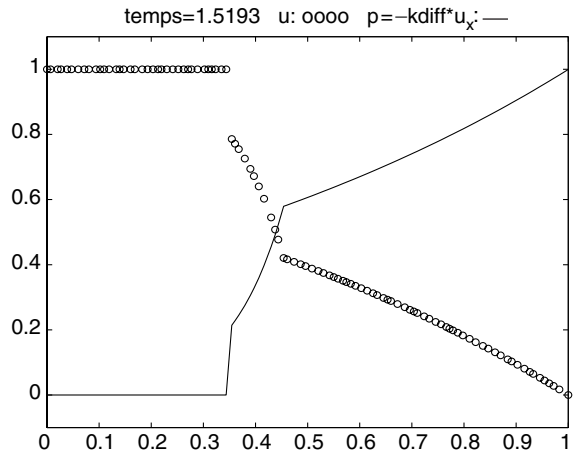

Fig. 12. Problem (72), Time $= T_6$, 100 boxes.

Table 2
Table of convergence rates for the second test-case (72)

Time	Conv. rate (u), 50/100 and 100/200	Conv. rate ($p = -\varepsilon u_x$), 50/100 and 100/200
$T_1 = 0.084$	0.65, 0.74	6.48, 4.83
$T_2 = 0.175$	1.06, 0.89	0.94, 0.76
$T_3 = 0.238$	1.17, 0.96	1.60, 0.98
$T_4 = 0.350$	1.41, 0.99	1.55, 1.15
$T_5 = 0.525$	1.63, 0.96	1.25, 1.00
$T_6 = 1.519$	1.58, 0.94	1.58, 0.94

5.3.2. Test-case of Noye and Tan

We consider the test proposed in [21] which consists of the deplacement of a 2D Gaussian pulse, initially centered at $(x_0, y_0) = (0.5, 0.5)$, and propagated by the convection–diffusion equation

$$u_t + c \cdot \nabla u - (\varepsilon_1 u_{xx} + \varepsilon_2 u_{yy}) = 0$$

along the diagonal of the square $\Omega = [0, 2]^2$, during 1.25 s. The Dirichlet boundary conditions are the values of the exact solution on the boundary. The diffusion coefficients are $\varepsilon_1 = \varepsilon_2 = 0.01$, and the velocity is $\vec{c} = (0.8, 0.8)$. The exact solution of this problem is given by

$$g(x, y, t) = \frac{1}{4t + 1} \exp\left[-\frac{(x - c_1 t - x_0)^2}{\varepsilon_1 (4t + 1)} - \frac{(y - c_2 t - y_0)^2}{\varepsilon_2 (4t + 1)} \right]$$

We compare our results with those of Turner and Truscott [27]. The error at time t_0 is the mesh dependent error denoted by $e_{\mathrm{TT}}(t_0)$, defined by

Table 3
Comparison between the finite-volume method and the ADI-box-scheme

Mesh size	Mesh 1	Mesh 2	Mesh 3
Peclet number	2.6667	1.2698	0.8
Box peak height	0.1452	0.1636	0.1660
TT peak height		0.1382	0.1518
Box e_{TT}	2.2727073e−4	1.0844153e−5	9.4819593e−7
TT e_{TT}		4.975446e−5	1.424502e−5
Box L^2 error	0.0103	2.2239e−3	4.9213e−4
L^2 Conv. rate		2.0661	3.2644

$$e_{TT}(t_0) = \frac{1}{N_x N_y}\sqrt{\frac{\sum_{i=1}^{N_x}\sum_{j=1}^{N_y}(u(i,j) - g(x(i),y(j),t_0))^2}{\sum_{i=1}^{N_x}\sum_{j=1}^{N_y}u(i,j)^2}} \tag{74}$$

where N_x and N_y are respectively the number of horizontal and vertical nodes. The numerical solution is computed on three different regular meshes:

- a coarse mesh of 961 nodes (31 points along x and y axis) (mesh 1),
- a medium mesh of 4096 nodes (64 points along x and y axis) (mesh 2),
- a fine mesh of 10 201 nodes (101 points along x and y axis) (mesh 3).

The coarse mesh (mesh 1) is selected to obtain a Peclet number $Pe \geqslant Pe_0 = 2.5$ giving that the upwind coefficient D_u is not equal to zero. In contrast, $D_u = 0$ for the two last meshes, mesh 2 and mesh 3, used by Turner and Truscott. We compare the peak level and the quantity e_{TT} at final time $T = 1.25$, with the values obtained by a Control Finite-Volume Method used by Turner and Truscott on meshes 2 and 3. We subscript the results with the suffixes *Box* for the box-scheme, and TT for the Turner and Truscott scheme. Additional results are given in the case of the ADI box-scheme. These results are presented in Table 3. The peak height of the exact solution is 1 at $T = 0$, and $1/6 \simeq 0.1667$ at the final time $T = 1.25$.

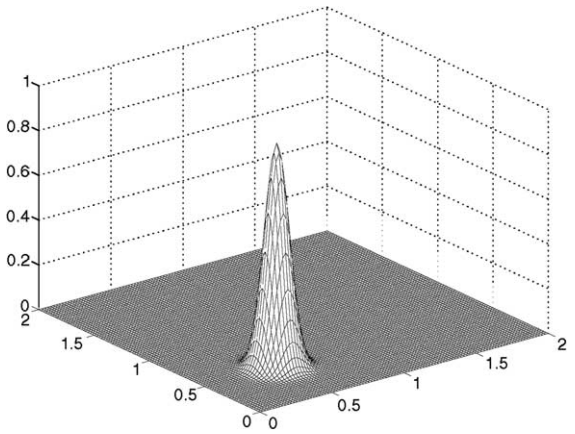

Fig. 13. Initial exact solution.

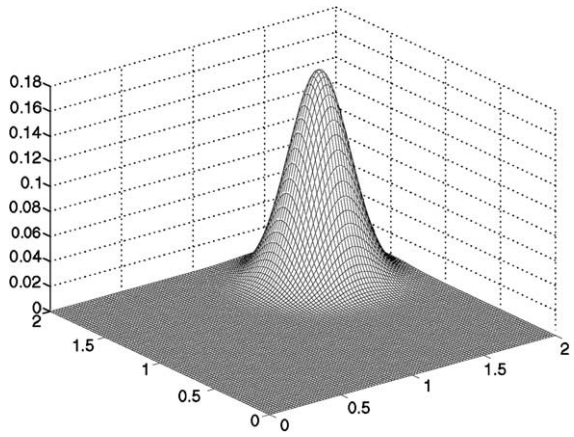

Fig. 14. Final exact solution.

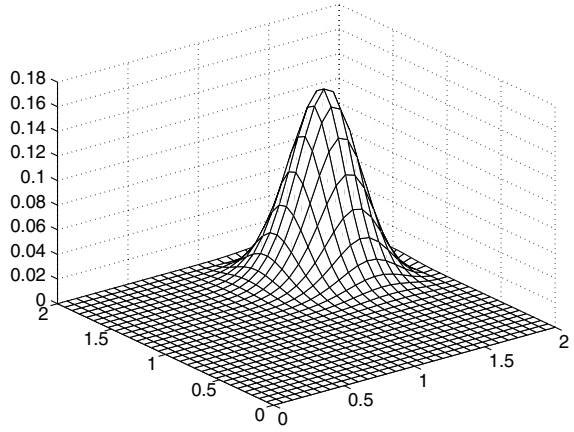

Fig. 15. Computed solution for 31 points at final time $T = 1.25$.

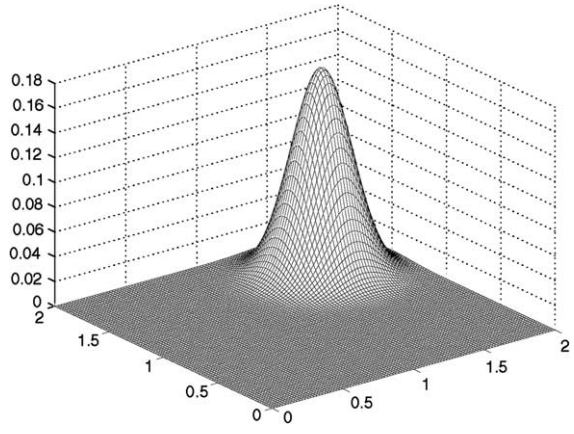

Fig. 16. Computed solution for 101 points at final time $T = 1.25$.

The ADI box-scheme gives good results, in comparison with those of Turner and Truscott. For this problem, the rate of the L^2 error is 2 when measured between mesh 1 and mesh 2 and around 3 when measured between mesh 2 and mesh 3. Here, we display results for the velocity u only. Note that one could use the value of the gradient to enhance the accuracy of the solution. We have plotted in Figs. 13 and 14, the exact solution at the initial and final times and in Fig. 15–18, the solutions computed with mesh 1 and mesh 3. The two last figures, Figs. 19 and 20 display the difference between the exact and the solutions computed with mesh 1 and mesh 3. Figs. 17 and 19 show the dissipation and dispersion of the scheme at low level spatial resolution in the cross direction $x = y$.

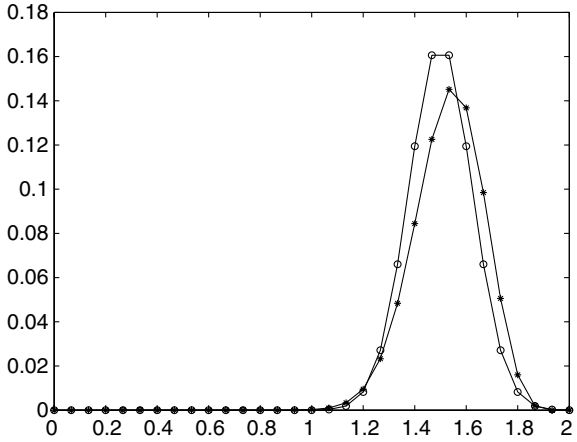

Fig. 17. Diagonal plots of exact solution u: ○ and computed solution u_h: ∗, for 31 points at $T = 1.25$.

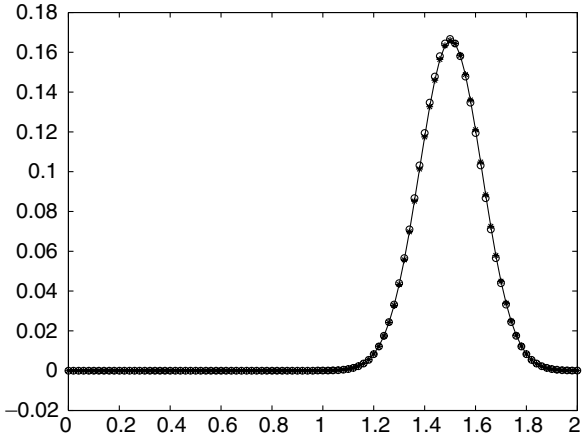

Fig. 18. Diagonal plots of exact solution u: ○ and computed solution u_h: ∗, for 101 points at $T = 1.25$.

5.4. Test-case of Balaguer et al.

The second test is given by Balaguer et al. [1]. We compute the numerical solution of the following equation

$$u_t + (v_0 + \lambda_y)u_x - D(u_{xx} + u_{yy}) = 0 \tag{75}$$

with Dirichlet boundary conditions given by the exact solution

$$u(x, y, t) = \frac{\Delta M}{4\pi Dt(1 + \lambda^2 t^2/12)} \exp\left(-\frac{(x - \bar{x} - 0.5\lambda yt)^2}{4Dt(1 + \lambda^2 t^2/12)} - \frac{y^2}{4Dt} \right) \tag{76}$$

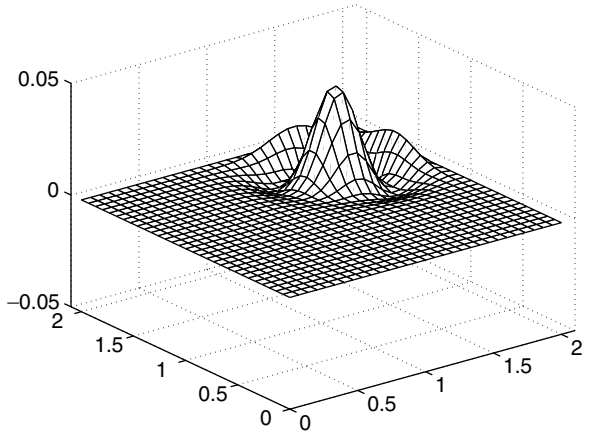

Fig. 19. Error between exact and computed solutions for 31 points.

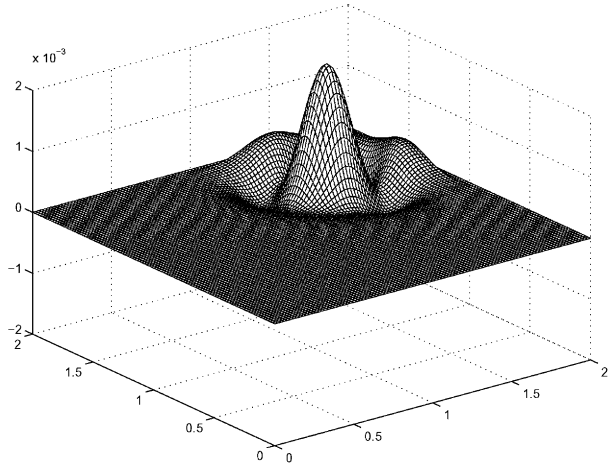

Fig. 20. Error between exact and computed solutions for 101 points.

Table 4
Computed results at final time $T = 4800$ for meshes 1, 2 and 3 on Balaguer's et al. test-case

Mesh size	Mesh 1	Mesh 2	Mesh 3
h	200	100	50
N_x	201	401	801
N_y	21	41	81
Time step	80	40	20
Peak height	0.3643	0.4793	0.4955
L^2 error	59.5037	20.8254	4.6216
Convergence rate		1.5146	2.1719

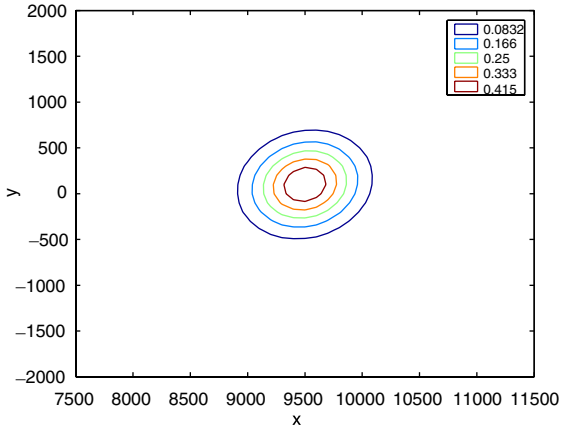

Fig. 21. Initial contour plot, $h = 100$.

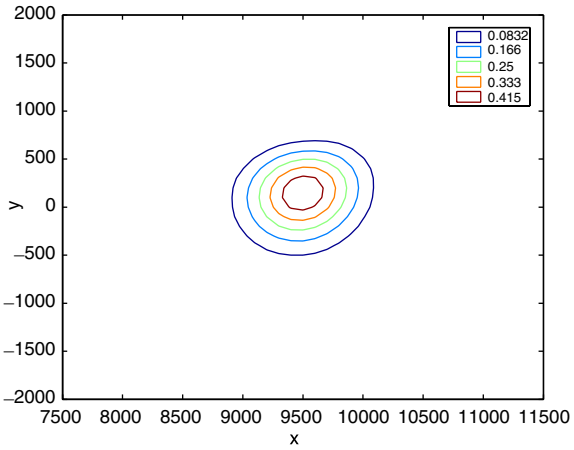

Fig. 22. Computed contour plot, $h = 100$.

where v_0 is the velocity on $y = 0$, λ is the slope of the velocity profile and D is a positive constant. ΔM is a point source of mass at $x = x_0$, $y = 0$ and $t = 0$. $\bar{x}$ is defined by $\bar{x} = x_0 + v_0 t$. We take the

computational domain $\Omega = [-20\,000; 20\,000] \times [-2000; 2000]$, the initial time t_{ini} is equal to $t_{\text{ini}} = 2400$, $\Delta M = 4\pi D t_{\text{ini}}(1 + \lambda^2 t^2/12)^{1/2}$ so that the initial peak concentration is equal to 1. We take the following parameters: $x_0 = 7200$, $v_0 = 0.5$, $\lambda = 5 \times 10^{-5}$, $D = 10$. In the two first cases, the spatial step size is $h = h_x = h_y = 200$, (resp. 100) and the CFL number is 0.24. We compute the solution during a time interval of 2400. The final time is $t_{\text{final}} = 4800$. The final peak height of the exact solution is 0.4991 (Table 4).

Note that the velocity $(c_1, c_2) = (v(y), 0)$ is non-symmetric, with $v(y) = v - 0 + \lambda y$. The initial pulse is convected in the x-direction only. The Peclet number along x, $Pe_x = \frac{|c_1|h_x}{2\varepsilon}$ is non-constant. One has $4 \leqslant Pe_x \leqslant 6$ in the case $h = 200$, and $2 \leqslant Pe_x \leqslant 3$ in the case $h = 100$. In this last case, the upwind coefficient $D_{u,x}$ varies on each horizontal edge between 0 and 1/30. The vertical coefficients Pe_y and $D_{u,y}$ vanish everywhere.

In a third case, we take a spatial step-size of $h = 50$. The upwind coefficient D_u vanishes everywhere. The convergence rates are between 1.5 and 2. We have plotted some numerical results in Figs. 21–24.

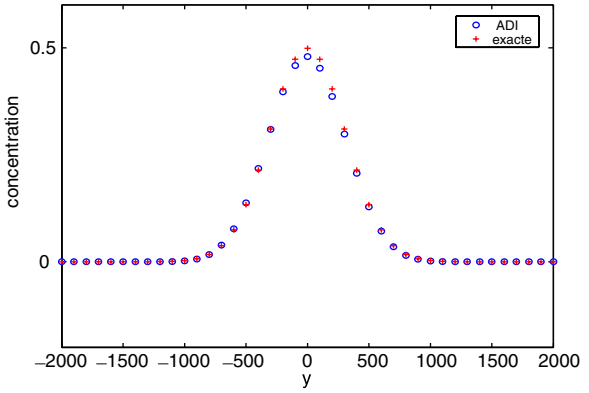

Fig. 23. Cross section in $x = 9600$, $h = 100$.

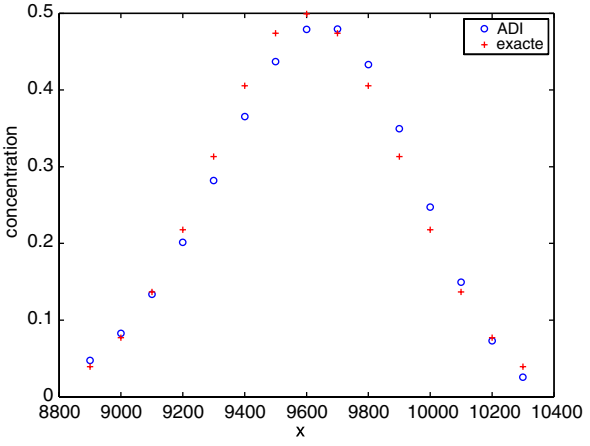

Fig. 24. Cross section in $y = 0$, $h = 100$.

6. Conclusion

In this work, we have focused on the basic design of a mixed box-scheme for 1D convection–diffusion equations. We stress that the design is the same in hyperbolic or parabolic regions. The scheme has a practical accuracy depending on the value of the local Peclet number. Here, the tuning of the upwind parameters is independent of the local behaviour of the solution. Future work will be devoted to the study of non-linear control of the upwind coefficients D_u, D_p, in order to detect and prevent dispersive oscillations [12]. In addition, the extension to 2D problems with irregular meshes is in progress.

Acknowledgements

The authors thank gratefully J. Roberts for her interest and constructive critics on this paper.

References

[1] Balaguer A, Conde C, Lòpez JA, Martiñez V. A finite volume method with a modified ENO scheme using a Hermite interpolation to solve advection–diffusion equations. Int J Numer Methods Eng 2001;50:2339–71.
[2] Carey GF, Spotz WF. Higher order mixed methods. Commun Numer Methods Eng 1997;13:553–64.
[3] Carpentier R, de la Bourdonnaye A, Larrouturou B. On the derivation of the modified equation for the analysis of linear numerical methods. Math Model Numer 1997;31(4):459–70.
[4] Casier F, Deconninck H, Hirsch C. A class of central bidiagonal schemes with implicit boundary conditions for the solution of Euler's equations. AIAA-83-0126, 1983.
[5] Chattot JJ. Box-schemes for first order partial differential equations. In: Advances in comp fluid dynamics. Gordon Breach Publ; 1995. p. 307–31.
[6] Chattot JJ, Malet S. A "box-scheme" for the Euler equations. In: Lecture Notes in Math, vol. 1270. Springer-Verlag; 1987. p. 82–99.
[7] Courbet B. Schémas à deux points pour la simulation numérique des écoulements. Rech Aérospatiale 1990;4:21–46.
[8] Courbet B. Etude d'une famille de schémas boîte à deux points et application à la dynamique des gaz monodimensionnelle. Rech Aérospatiale 1991;5:31–44.
[9] Courbet B, Croisille JP. Finite volume box schemes on triangular meshes. Math Model Numer 1998;32(5):631–49.
[10] Croisille J-P. Finite volume box schemes and mixed methods. Math Model Numer 2000;34(5):1087–106.
[11] Croisille J-P. Keller's box-scheme for the one-dimensional stationary convection–diffusion equation. Computing 2002;68:37–63.
[12] Croisille J-P. A high order accurate box-scheme for the one dimensional convection–diffusion equation, Preprint 2002, Laboratoire de mathématiques de Metz.
[13] Croisille J-P, Greff I. Some box-schemes for elliptic problems. Numer Methods Partial Differ Equat 2002;18:355–73.
[14] Croisille J-P, Greff I. A box scheme for convection–diffusion equations. In: Proc of the 3. ISFVMCA, Porquerolles, Hermes, 2002.
[15] Douglas J, Gunn JE. A general formulation of alternating direction methods; Part I. Parabolic and hyperbolic problems. Numer Math 1964;6:428–53.
[16] Douglas J, Rachford HH. On the numerical solution of heat conduction problems in two and three space variables. Trans Am Math Soc 1956;82:421–39.
[17] Hedstrom GW. Models of difference schemes for $u_t + u_x = 0$ by partial differential equations. Math Comput 1975;29(132):969–77.

[18] Greff I. Schémas boîte, étude théorique et numérique, PhD, Université de Metz, 2003. Available from: <http://www.mmas.univ-metz.fr>.
[19] Keller HB. A new difference scheme for parabolic problems. In: Hubbard B, editor. Numerical solutions of partial differential equations, vol. II. New-York: Academic Press; 1971. p. 327–50.
[20] Lele SK. Compact finite-difference schemes with spectral-like resolution. J Comput Phys 1992;103:16–42.
[21] Noye BJ, Tan HH. Finite difference methods for solving the 2D convection–diffusion equation. Int J Numer Methods Fluids 1989;(9):75–98.
[22] Peaceman DW, Rachford HH. The numerical solution of parabolic and elliptic equations. SIAM J 1955;3:28–41.
[23] Rigal A. High order difference methods for unsteady 1D diffusion–convection problems. J Comput Phys 1994;114:59–76.
[24] Smith R. Optimal and near optimal advection–diffusion finite difference schemes, II—Unsteadiness and non-uniform grid. Proc Roy Soc Lond A 2000;456:489–502.
[25] Strickwerda J. Finite difference schemes and partial differential equations. Wadsworth & Brooks/Cole Publ; 1989.
[26] Tolstykh AI. High accuracy non-centered compact difference schemes for fluid dynamics applications. World Scientific; 1994.
[27] Truscott SL, Turner IW. An investigation of spatial and temporal weighting schemes for use in unstructured mesh control volume finite element methods. ANZIAM J 2003;44(E):C759–79.
[28] Wornom SF. Application of compact difference schemes to the conservative Euler equations for one-dimensional flows. NASA Tech Mem 83262, 1982.
[29] Wornom SF, Hafez MM. Implicit conservative schemes for the Euler equations. AIAA J 1986;24(2):215–33.
[30] Zhang J. An explicit fourth-order compact finite difference scheme for three dimensional convection–diffusion equation. Commun Numer Methods 1998;14:263–80.